Molecular and biophysical basis of glutamate and trace metal modulation of voltage-gated Ca$_v$2.3 calcium channels

Aleksandr Shcheglovitov,[1] Iuliia Vitko,[1] Roman M. Lazarenko,[1] Peihan Orestes,[2,3] Slobodan M. Todorovic,[2,3] and Edward Perez-Reyes[1,3]

[1]Department of Pharmacology, [2]Department of Anesthesiology, and [3]Neuroscience Graduate Program, University of Virginia, Charlottesville, VA 22908

Here, we describe a new mechanism by which glutamate (Glu) and trace metals reciprocally modulate activity of the Ca$_v$2.3 channel by profoundly shifting its voltage-dependent gating. We show that zinc and copper, at physiologically relevant concentrations, occupy an extracellular binding site on the surface of Ca$_v$2.3 and hold the threshold for activation of these channels in a depolarized voltage range. Abolishing this binding by chelation or the substitution of key amino acid residues in IS1–IS2 (H111) and IS2–IS3 (H179 and H183) loops potentiates Ca$_v$2.3 by shifting the voltage dependence of activation toward more negative membrane potentials. We demonstrate that copper regulates the voltage dependence of Ca$_v$2.3 by affecting gating charge movements. Thus, in the presence of copper, gating charges transition into the "ON" position slower, delaying activation and reducing the voltage sensitivity of the channel. Overall, our results suggest a new mechanism by which Glu and trace metals transiently modulate voltage-dependent gating of Ca$_v$2.3, potentially affecting synaptic transmission and plasticity in the brain.

INTRODUCTION

Voltage-gated calcium channels (VGCCs) play essential roles in all eukaryotes, allowing calcium to enter the cell in response to membrane depolarization. A variety of cellular processes including gene expression, synaptic transmission, and apoptosis are regulated by the dynamic concentration of intracellular calcium (Clapham, 2007). Thus, expression and function of VGCCs are under tight cellular control. The family of VGCCs is heterogeneous and, in mammals, consists of 10 members: L- (Ca$_v$1.1, Ca$_v$1.2, Ca$_v$1.3, and Ca$_v$1.4), P/Q- (Ca$_v$2.1), N- (Ca$_v$2.2), R- (Ca$_v$2.3), and T-type (Ca$_v$3.1, Ca$_v$3.2, and Ca$_v$3.3) (Catterall et al., 2005). In the brain, these channels mediate the following functions: L-type calcium channels were shown to be mainly responsible for regulating gene expression; N-, P/Q-, and R-type for synaptic transmission and plasticity; and T-type for pacemaker and burst firing of neurons (Zamponi, 2005). Of all the calcium channels, R-type channels are arguably the most mysterious subtype. Despite considerable investigation, its physiological role remains the least understood (Weiergräber et al., 2006). In many cases, they promote neuronal excitability, contributing to the induction of long-term potentiation (LTP) (Dietrich et al., 2003), triggering synaptic transmission (Wu et al., 1998; Gasparini et al., 2001) and generating both bursts of action potentials (APs) and plateau potentials (Kuzmiski et al., 2005; Metz et al., 2005; Tai et al., 2006; Park et al., 2010). In other cases, Ca$_v$2.3 channels attenuate neuronal excitability by dampening activation of NMDA receptors in the spines of CA1 pyramidal neurons (Bloodgood and Sabatini, 2007) and depressing the induction of LTP after trains of back-propagating APs (Yasuda et al., 2003). Ca$_v$2.3 channels are widely distributed throughout the brain (Weiergräber et al., 2006) and are considered to be the molecular correlate for R-type current in native cells (Piedras-Rentería and Tsien, 1998; Tottene et al., 2000; Sochivko et al., 2002). These channels were shown to be indirectly modulated by glutamate (Glu) and acetylcholine through a PKC-dependent pathway (Stea et al., 1995; Bannister et al., 2004; Kamatchi et al., 2004; Tai et al., 2006; Park et al., 2010; but see Giessel and Sabatini, 2010).

Transition metals play fundamental roles in a variety of vital cellular processes, serving as cofactors in several enzymes, stabilizers of protein structures, and regulators of neuronal excitability (Mathie et al., 2006). A significant increase in trace metal content in the brain has been detected in association with several pathological conditions, including epilepsy, stroke, Alzheimer's, Parkinson's,

The Rockefeller University Press $30.00
J. Gen. Physiol. Vol. 139 No. 3 219–234
www.jgp.org/cgi/doi/10.1085/jgp.201110699

219

and Creutzfeldt–Jakob diseases (Frederickson et al., 2005; Barnham and Bush, 2008). Additionally, aging-dependent accumulation of Zn^{2+} and Cu^{2+} in the brain correlates with a higher risk for the development of neurological disorders (Barnham and Bush, 2008). In contrast to other biologically relevant divalent cations, such as Ca^{2+} and Mg^{2+}, free concentrations of trace metals in the brain are extremely low and strictly regulated by a variety of metalloproteins (Valko et al., 2005). Concentrations of Zn^{2+} and Cu^{2+} in a healthy brain are estimated to be around 70–150 µM (Mathie et al., 2006). Although most of the ions (>95%) are protein bound, local free, or loosely bound, concentrations of Zn^{2+} and Cu^{2+} can reach 30 µM (Frederickson et al., 2005) and 1.7 µM (Mathie et al., 2006), respectively. Pools of "chelatable" Zn^{2+} and Cu^{2+} have been identified in the synaptic vesicles of specific (gluzinergic and glucupergic) subsets of glutamatergic neurons in the cortex, hippocampus, striatum, and amygdala (Mathie et al., 2006), and are released into the synaptic cleft upon membrane depolarization in a Ca^{2+}-dependent manner (Barnham and Bush, 2008). Identification of the molecular targets for these released metal ions will provide novel insights into neuronal viability, synaptic plasticity, and excitability, as well as a deeper understanding of mechanisms of development of various neurological disorders (Frederickson et al., 2005; Barnham and Bush, 2008).

Various proteins and amino acids have submicromolar affinity to Zn^{2+} and Cu^{2+} (Dawson et al., 1986; Karlin, 1993; Regan, 1993). In contrast, only a few ion channels and receptors are reported to possess this capacity, including NMDA receptors (Paoletti et al., 2009), $Ca_v3.2$ calcium channels (Jeong et al., 2003; Nelson et al., 2007a,b; Traboulsie et al., 2007), $GABA_A$ receptors (Hosie et al., 2003), and BK K^+ potassium channels (Ma et al., 2008). The sensitivity of $Ca_v2.3$ channels toward Ni^{2+} has been known since their discovery (Ellinor et al., 1993; Soong et al., 1993; Zhang et al., 1993; Zamponi et al., 1996). However, it is unknown whether these channels are sensitive to physiologically relevant concentrations of zinc and copper. Studying the effect of Zn^{2+} and Cu^{2+} on $Ca_v2.3$, we discovered, surprisingly, that Glu and glycine (Gly) can substantially potentiate activity of these channels by shifting their gating toward more hyperpolarized voltages. The effect arose from the ability of amino acid residues to chelate trace metals, binding to the extracellular surface of the channel and blunting its voltage sensitivity. As a result of mutagenesis studies and detailed biophysical analysis of ion currents, we have identified a molecular determinant responsible for this sensitivity and described a plausible biophysical mechanism underlying it. Overall, our data reveal previously unknown properties of $Ca_v2.3$ calcium channels and suggest a new and potentially important mechanism through which these channels might influence synaptic transmission and plasticity in the brain.

MATERIALS AND METHODS

Site-directed mutagenesis
A human $Ca_v2.3d$ cDNA (available from GenBank/EMBL/DDBJ under accession no. L27745) contained in pcDNA3 vector was mutated using the single-overlap extension technique. The primers were obtained from Operon and used without purification. The full-length cDNA contained in pcDNA3 was reassembled using a ClaI/XhoI fragment of the mutated clone. The sequence of this fragment was verified by automated sequencing.

Calibration of free Zn^{2+} and Cu^{2+} concentrations in Tricine solution
Fluorescent signals were measured on a fluorescent reader (FlexStation; Molecular Devices). After recording the baseline for 20 s, 25 µl of solutions containing varying concentrations of Zn^{2+} or Cu^{2+} was added using integrated fluidics to a 96-well plate containing 125 µl of dye. Signals were acquired every 2 s (excitation/emission, nm): 506/550 for Newport Green DCF and 370/520 for Mag-Fura-2. Each experiment was performed in triplicate, and the data represent the mean ± SEM from three experiments. Free Zn^{2+} was measured using 3 µM Newport Green DCF dye. Note that the solutions used for this experiment did not contain TEA and contained either 1 mM HEPES or 10 mM Tricine and KCl to adjust the ionic strength to 0.1 M, pH 7.4. To avoid trace metal contamination, we strictly followed the methods described by Aslamkhan et al. (2002). Because the background fluorescent signals measured in these HEPES and Tricine solutions were similar (Fig. 4), we conclude that this HEPES solution was not contaminated with trace metals, and that concentrations of free and added Zn^{2+} or Cu^{2+} were equal. Fluorescence responses in a range of Zn^{2+} concentrations from ∼1 to 40 µM in HEPES were fitted with the Hill equation ($K_d = 10^{-5.4}$ M and $n_H = 1.3$). Free concentrations of Zn^{2+} in Tricine solution were estimated by rearranging the Hill equation and solving for concentration using the fluorescence signal observed in Tricine and the K_d and n_H values acquired in HEPES solution. We then used the Solver function in the MaxChelator program (Winmaxc version 2.40 available at http://maxchelator.stanford.edu) (Patton et al., 2004) to predict free Zn^{2+} using $K_1 = 10^{-5}$ M for the M + L ↔ ML equilibrium and $K_2 = 10^{-3}$ M for the ML + L ↔ ML_2 equilibrium. The predicted values matched the experimentally determined values, indicating that the empirically determined K_d value was correct (Paoletti et al., 1997). Free Cu^{2+} concentrations in Tricine solution were measured using 3 µM Mag-Fura-2. As described for Zn^{2+}, free concentrations of Cu^{2+} were calculated using the Hill equation (HEPES, $K_d = 10^{-6.6}$ M and $n_H = 1.5$). We then iteratively changed the K_1 and K_2 of Tricine for Cu^{2+} until Solver's predictions matched the experimental results. These values converged when $K_1 = 10^{-6.3}$ M and $K_2 = 10^{-3.3}$ M. Similar results were obtained in MOPS-buffered solutions, so the results were pooled. We also measured the fluorescent responses to free Cu^{2+} concentrations that were calculated by Solver for a 1-mM citrate buffer, pH 7.4. The observed quenching of the Mag-Fura-2 fluorescence by this predicted free Cu^{2+} was similar to that observed in HEPES ($K_d = 10^{-6.1}$ M and $n_H = 1.0$), thereby confirming our estimates of free Cu^{2+}.

Dorsal root ganglion (DRG) neurons
Acutely dissociated DRG cells were prepared from adolescent (60–150 g, 3–8-wk-old) Sprague Dawley rats as described previously (Todorovic and Lingle, 1998; Nelson et al., 2005). Cells were plated onto uncoated glass coverslips and incubated for 30 min at room temperature. Before the experiments, coverslips were incubated for 10 min in the Tyrode's solution supplemented with 10 µg/ml IB_4 conjugated to green FITC (Sigma-Aldrich) and subsequently rinsed three times with the external solution. All experiments were performed at room temperature. Currents were recorded using the following external and internal solutions

(in mM): 125 NaCl, 20 TEA-Cl, 3 KCl, 2 $MgCl_2$, 5 $BaCl_2$, 4 4-AP, and 10 HEPES or Tricine, pH 7.4 with HCl, and 125 CsCl, 10 BAPTA, 2 $CaCl_2$, 1 $MgCl_2$, 4 Mg-ATP, 0.3 Li-GDPβ$_S$, and 10 HEPES, pH 7.2 with CsOH, respectively. The recording chamber was constantly perfused with the extracellular solution at 1 ml/min. To isolate R-type current, the external solution was supplemented with the following blockers: 1.5 µM ω-conotoxin MVIIC, 0.1 µM ω-conotoxin-GVIA, 0.05 µM ω-agatoxin IVA, 10 µM nimodipine, and 0.5 µM TTA-P2 in 0.1 mg/ml cytochrome c.

Currents in these cells were measured at room temperature (∼22°C) using MultiClamp 700B amplifier, Digidata 1322A, and pClamp 9.2 software (Molecular Devices). Data were filtered at 2 kHz and digitized at 5 kHz. Access resistance was in the range of 5 to 10 MΩ. Series resistance was 50–60% compensated. Membrane capacitance and leak current were compensated using the P/5 on-line leak subtraction procedure.

Human embryonic kidney (HEK) cells

HEK-293 cells (CRL-1573; American Type Culture Collection) were grown in DMEM/F-12 (Invitrogen) supplemented with 10% fetal calf serum, 100 U/ml penicillin G, and 0.1 mg/ml streptomycin. Cells were transiently transfected with plasmid DNAs encoding Ca$_v$2.3d (Schneider et al., 1994), Ca$_v$2.2 or mutants (1 µg), human β2a (1 µg; available from GenBank/EMBL/DDBJ under accession no. AF423189), rabbit α$_2$δ1 (1 µg), and green fluorescent protein (GFP; 0.25 µg; pGreen Lantern; Invitrogen), or Ca$_v$3.2 (3 µg) and GFP (0.25 µg) using JET-PEI (MP Biomedicals). GFP$^+$ cells were recorded 24–48 h after transfection.

Electrophysiological experiments were performed using the conventional patch-clamp technique in the whole cell configuration. Currents were recorded at room temperature (∼22°C) using MultiClamp 700B amplifier with Digidata 1322A and pClamp 9.2 software (Molecular Devices). Data were filtered at

2 kHz and digitized at 5 kHz. Access resistance and cell capacitance were measured using the built-in Clampex Membrane Test function. The average access resistance was around 4 MΩ. Data from cells where the access resistance exceeded 5.5 MΩ were discarded. Series resistance was constantly monitored and compensated between protocols to 70% (prediction and correction; 10-µs lag), resulting in maximal residual voltage error below 1.6 mV during measurement of the I-V relationship. In experiments where gating currents were measured, data were filtered at 10 kHz (−3 dB, four-pole Bessel) and digitized at 50–100 kHz, and P/−8 protocol was applied for leak and capacitance compensation. Currents were recorded using the following external solutions (in mM): 1 (or 5) $CaCl_2$, 171 (or 166) TEA-Cl, and either 10 HEPES or Tricine, pH adjusted to 7.4 with TEA-OH. Pipettes for recordings (2–3 MΩ) were filled with internal solution of the following composition (in mM): 125 CsCl, 10 BAPTA, 2 $CaCl_2$, 1 $MgCl_2$, 4 Mg-ATP, 0.3 Li-GDPβ$_S$, and 10 HEPES, pH adjusted to 7.2 with CsOH. The recording chamber was constantly perfused with the extracellular solution at 1 ml/min. The complete solution exchange was achieved in ∼40–60 s; therefore, the apparent on-rates are dominated by bath exchange.

Data analysis and statistics

Data were analyzed using Clampfit 9.2 (Molecular Devices), MS Excel 2007 (Microsoft), and Prism 5.01 (GraphPad). Smooth curves in the figures represent fits to the average data, whereas the mean values in the table were calculated from fits to individual cells. Data are reported as the mean ± SEM. We used either one-way ANOVA, to compare multiple mean values, or a paired Student's t test when evaluating the effect of acute application of Tricine or trace metals. The voltage dependence of activation (m$_∞$; midpoint, V$_{1/2}$; slope, k) was determined by fitting the peak I-V data from each cell with a Boltzmann-Goldman–Hodgkin–Katz (GHK) equation:
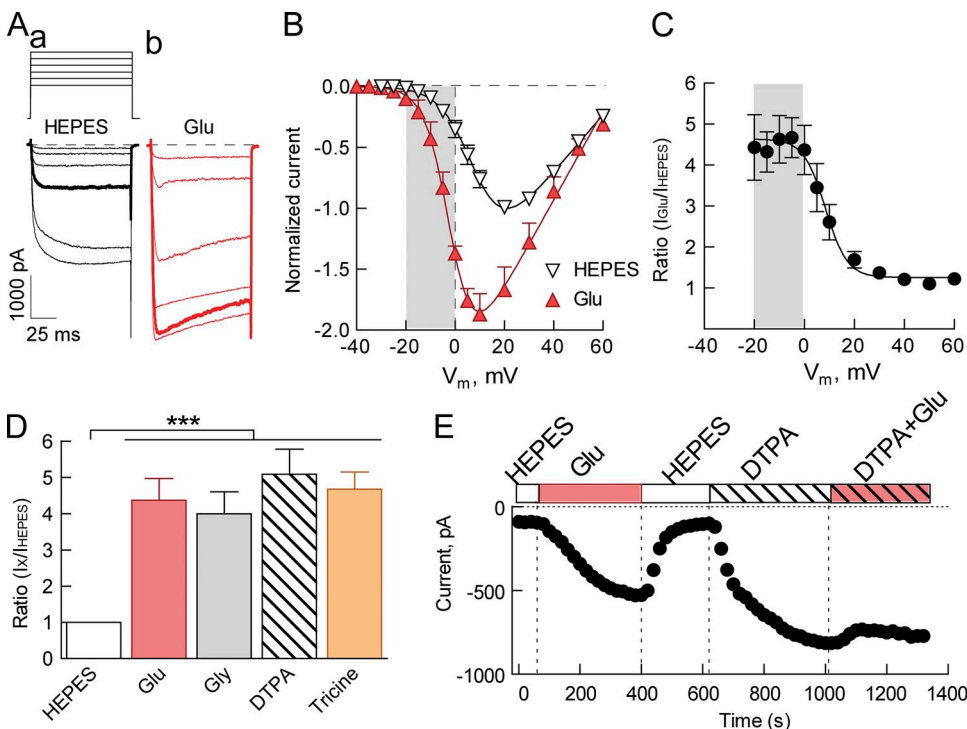
Figure 1. Neurotransmitter amino acids potentiate current through Ca$_v$2.3 channels by acting as trace metal chelators. (A) Representative current traces recorded in response to the I-V protocol (V$_{hold}$ = −90 mV; depolarizations to −15, −10, −5, 0, 10, and 20 mV) in a standard HEPES-buffered solution, containing 5 mM Ca^{2+} as a charge carrier, before (a) and after the addition of 200 µM Glu (b). Highlighted current traces elicited in response to 0-mV voltage step. (B) Normalized peak current I-V relationships measured in control HEPES and Glu-containing solutions. Data from each cell were fitted with GHK Eq. 1 (HEPES: V$_{1/2}$=19.4±1.9 and k = 7.4 ± 0.2 mV; Glu: V$_{1/2}$ = 5.4 ± 2.0 and k = 5.9 ± 0.3 mV; **, P < 0.001 by paired Student's t test for both parameters; $n = 5$). (C) Voltage dependence of the potentiating effect of Glu on Ca$_v$2.3. Ratio of peak current amplitudes (I$_{Glu}$/I$_{HEPES}$) at each potential plotted as a function of potential. (D) Potentiating effect of 200 µM Glu ($n = 5$), 200 µM Gly ($n = 4$), 100 µM DTPA ($n = 11$), and 10 mM Tricine ($n = 8$) on Ca$_v$2.3 currents elicited by the test pulses to −15–0 mV (***, P < 0.0001 by one-way ANOVA). (E) Time course of changes in the peak current amplitude induced by the sequential application of the indicated solutions measured at −20 mV. Note that the effect of Glu on Ca$_v$2.3 is abolished by coapplication of DTPA.

$$I(V, Ca_i, Ca_o) = \frac{P_{Ca} Z_{Ca}^2 F^2 V}{RT} \frac{(Ca_i - Ca_o)\exp(-Z_{Ca}FV/RT)}{1 - \exp(-Z_{Ca}FV/RT)} \frac{1}{1 + \exp[(V_{1/2} - V)/k]},$$ (1)

where P_{Ca} is the permeability to calcium ions (cm/s), Z is their valence (2), F is the Faraday constant, R is the gas constant, T is the temperature (K), V is the test potential (V), and Ca_i and Ca_o are the intracellular and extracellular concentrations of Ca^{2+} (M), respectively. For display purposes, the voltage dependence of activation was calculated as the ratio of peak current amplitudes (I) observed at each voltage to the instantaneous value calculated with the GHK equation (I_{GHK}), and then fit with the Boltzmann equation. Level of steady-state inactivation at different voltages was calculated as a ratio of currents (I/I_{max}) measured at +30 mV after 15-s-long conditioning prepulses.

Reagents
Solutions were prepared at the time of the experiments from fresh stocks in distilled water (in mM): 250 $CuCl_2$, 250 $ZnCl_2$, 500 diethylenetriamine pentaacetic acid (DTPA), 10 Glu, and 10 Gly. All chemicals were purchased from either Thermo Fisher Scientific or Sigma-Aldrich.

RESULTS

Excitatory amino acids modulate gating of $Ca_v2.3$ channels acting as trace metal chelators
Although Glu is well known as an excitatory neurotransmitter in the brain, its ability to serve as a trace metal chelator is often neglected (pK$_a$ 5.5 and 7.9 for Zn^{2+} and Cu^{2+}, respectively; Dawson et al., 1986). Studying the

effect of Glu on calcium channels, we revealed that Glu can profoundly modulate gating of $Ca_v2.3$ calcium channels, by acting as a chelator (Fig. 1). Supplementation of a standard HEPES-based bath solution with 200 µM Glu led to the significant potentiation of Ca^{2+} currents measured at negative voltages and an ∼15-mV leftward shift of the I-V relationship (Fig. 1, A and B). The maximal increase in current amplitude (4.4-fold) was detected in the range of potentials from −20 to 0 mV and gradually decreased with further depolarization (Fig. 1 C). A similar effect on $Ca_v2.3$ was recorded upon the application of either 200 µM Gly or 100 µM DTPA in the HEPES bath solution and after substitution of HEPES with Tricine (10 mM; Fig. 1 D). Consistent with its action as a chelator, the effect of Glu was fast, reversible, and abolished by concomitant application of 100 µM DTPA (Fig. 1 E). Because Glu can also modulate the activity of $Ca_v2.3$ calcium channels indirectly through G protein–coupled receptors (Stea et al., 1995), we used Tricine, which possesses similar chelating properties, to isolate and study the chelation effect of Glu (Fig. 2). As with Glu, Tricine replacement for HEPES produced a strong stimulation of current at negative voltages (5.2-fold at −20 mV; Fig. 2, A–C). Upon Tricine application, activation gating of $Ca_v2.3$ channels was substantially shifted to more negative potentials (Fig. 2 D and Table 1), with no significant effect on either currents recorded at positive voltages or permeability (P_{Ca}) (Fig. 2 B and Table 1),
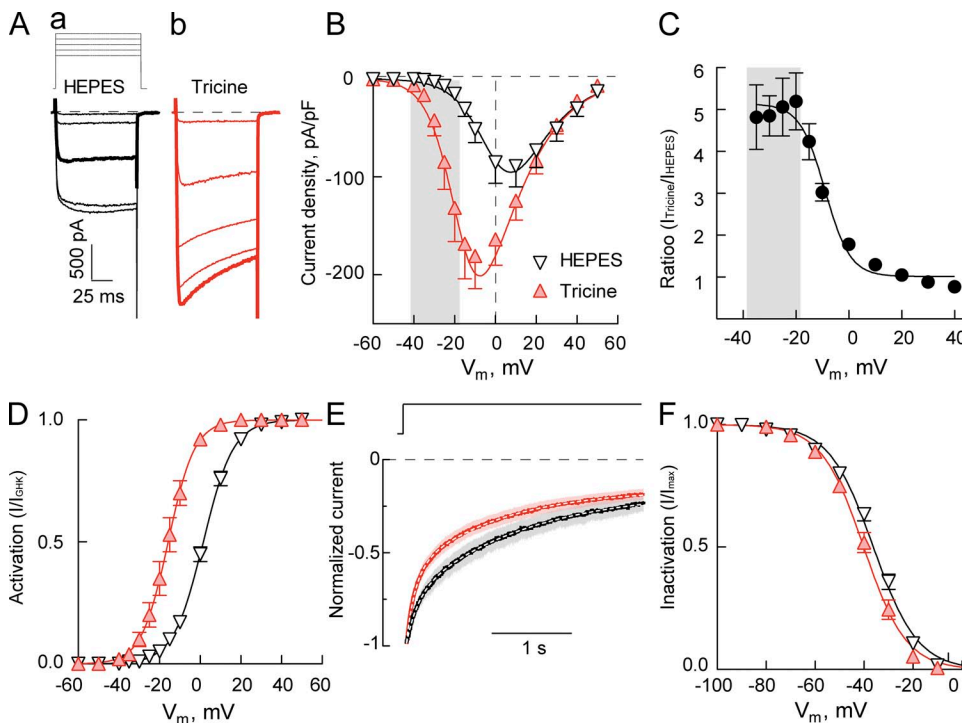
Figure 2. Tricine selectively affects the activation gating of $Ca_v2.3$. (A) Representative current traces recorded in response to the I-V protocol ($V_{hold} = -90$ mV; depolarizing pulses from −30 to +10 mV) in HEPES (a) and Tricine solutions (b) containing 1 mM Ca^{2+} as a charge carrier. Highlighted current traces recorded in response to a −10-mV voltage step. (B) Peak current I-V relationships obtained in HEPES- or Tricine-based extracellular solutions. Data were fitted with GHK Eq. 1 (Table 1). (C) Voltage dependence of the effect of Tricine on $Ca_v2.3$. Ratio of peak current amplitudes ($I_{Tricine}/I_{HEPES}$) at each potential plotted as a function of potential. (D) Voltage dependence of activation of $Ca_v2.3$ measured in HEPES- and Tricine-based extracellular solutions. (E) Normalized and averaged Ca^{2+} currents ± SEM (shaded area) recorded in response to prolonged (3-s) depolarizing pulse to −10 mV in HEPES and Tricine solutions. Recordings were fitted with double-exponential function: $I(t) = A_f \exp(-t/\tau_f) + A_s \exp(-t/\tau_s) + C$. Corresponding values and statistics are in Table 1. (F) Steady-state inactivation curves, measured at +30 mV after 15-s-long conditioning prepulses.

TABLE 1
Biophysical properties

Solution	Activation				Inactivation			Kinetics				
Ca$_v$2.3 WT	P$_{Ca(max)}$ ± SEM	V$_{1/2}$ ± SEM	k ± SEM	n	V$_{1/2}$ ± SEM	k ± SEM	n	A$_f$ ± SEM	τ$_f$ ± SEM	A$_s$ ± SEM	τ$_s$ ± SEM	n
HEPES	0.011 ± 0.003	1.5 ± 1.0[a]	7.2 ± 0.1[a]	8	−36.1 ± 1.1[b]	8.9 ± 0.2	8	−0.24 ± 0.05[b]	0.17 ± 0.02	−0.59 ± 0.04	1.5 ± 0.2	6
Tricine	0.010 ± 0.002	−15.6 ± 1.8	5.3 ± 0.2	12	−40.2 ± 1.2	8.2 ± 0.3	11	−0.38 ± 0.03	0.13 ± 0.01	−0.44 ± 0.02	1.2 ± 0.1	6
Zn 7 µM	0.005 ± 0.001	−2.4 ± 2.9[a]	7.1 ± 0.1[a]	4	−30.4 ± 1.8[a]	9.8 ± 0.5	6	−0.14 ± 0.01[a]	0.33 ± 0.08	−0.52 ± 0.06	2.4 ± 0.6	6
Cu 205 nM	0.007 ± 0.002	2.9 ± 1.2[a]	7.4 ± 0.1[a]	6	−26.8 ± 1.2[a]	9.7 ± 0.8	6	−0.18 ± 0.04[a]	0.21 ± 0.08	−0.48 ± 0.04	3.1 ± 0.4[b]	6
H179E/H181A												
HEPES	0.010 ± 0.002	−12.7 ± 1.0	5.0 ± 0.2	7	−42.9 ± 1.8	9.1 ± 0.4	6	−0.32 ± 0.04	0.14 ± 0.02	−0.59 ± 0.04	1.3 ± 0.1	5
Tricine	0.010 ± 0.001	−12.1 ± 1.1	5.2 ± 0.2	13	−41.2 ± 1.3	8.4 ± 0.2	8	−0.34 ± 0.03	0.14 ± 0.01	−0.55 ± 0.02	1.2 ± 0.1	5
Zn 7 µM	0.008 ± 0.002	−9.4 ± 0.9	6.0 ± 0.3	5	−36.0 ± 2.4	9.2 ± 0.8	4	−0.31 ± 0.04	0.23 ± 0.11	−0.65 ± 0.17	2.8 ± 1.1	3
Cu 205 nM	0.009 ± 0.002	−8.6 ± 1.9	5.6 ± 0.2	8	−37.2 ± 1.1	8.0 ± 0.4	6	−0.33 ± 0.02	0.20 ± 0.06	−0.64 ± 0.12	2.4 ± 0.7	5

All parameters were calculated for each cell and then averaged. Statistically significant differences are noted with footnotes and are by one-way ANOVA, compared to the values obtained in Tricine:

[a]P < 0.001.
[b]P < 0.5.

and a moderate effect on kinetics of inactivation (Fig. 2 E and Table 1) and steady-state inactivation (Fig. 2 F and Table 1).

We tested the specificity of the effect of trace metal chelators on activation gating of Ca$_v$2.3 by measuring the effect of Tricine on Ca$_v$2.2 and Ca$_v$3.2 channels (Fig. 3). The substitution of Tricine for HEPES produced no effect on either amplitude or voltage dependence of Ca$_v$2.2 (Fig. 3, A–C). However, it significantly stimulated the amplitude of Ca$_v$3.2 currents at all tested potentials, with no effect on activation gating (Fig. 3, D–F), similar to what was reported previously by Nelson et al. (2007a). This suggests that the effect of trace metals on activation gating is specific for Ca$_v$2.3 channels. Interestingly, results of these experiments also revealed the mid-voltage–activated nature of Ca$_v$2.3 channels (V$_{1/2}$ = −15.6 ± 1.8 mV; Fig. 2 B), as under identical recording conditions (1 mM Ca^{2+} as charge carrier in 10 mM Tricine), Ca$_v$3.2 and Ca$_v$2.2 channels activated at more negative (V$_{1/2}$ = −48.7 ± 1.2 mV; Fig. 3 F) and at more positive (V$_{1/2}$ = −3.8 ± 0.9 mV; Fig. 3 C) membrane potentials, respectively.

It was shown that Tricine efficiently chelates Zn^{2+} in the concentration range from 1 nM to 1 µM, with an empirically estimated K$_d$ of ∼10^{-5} M (Paoletti et al., 1997). Additionally, Tricine is a derivate of Gly (*N*-Tris (hydroxymethyl)methylglycine), which can bind Cu^{2+} with even higher affinity than Zn^{2+} (K$_d$ of 10$^{-8.1}$ M vs. 10^{-5} M, respectively; Dawson et al., 1986). This suggests that excitatory amino acids and Tricine could exert their effect on Ca$_v$2.3 by chelating trace amounts of Zn^{2+} and/or Cu^{2+}, which commonly reside in normal bath solutions (Kay, 2004). Indeed, the direct addition of 100 µM Zn^{2+} or Cu^{2+}, but not Fe^{2+}, to the Tricine-based extracellular solution substantially suppressed currents at negative potentials (not depicted). To study the mechanisms responsible for modulation of Ca$_v$2.3 calcium channels by trace metals and their chelators, we calibrated

free concentrations of Cu^{2+} and Zn^{2+} in Tricine-containing solution using fluorescent dyes Newport Green DCF (Fig. 4 A) and Mag-Fura-2 (Fig. 4 B). These dyes were selected based on their micromolar affinity for Zn^{2+} and Cu^{2+}, but low affinity for Ca^{2+} (Haugland, 2005). Free concentrations of Zn^{2+} and Cu^{2+} in Tricine were deduced by comparing the fluorescent signals measured in the absence of trace metal chelators to those obtained in 10 mM Tricine (Fig. 4). From these values, we deduced the K$_d$ for copper and zinc binding to Tricine, and then used the program MaxChelator (http://maxchelator .stanford.edu) to deduce free ion concentrations under a variety of conditions (Table 2).

We next assessed the effects of calibrated Zn^{2+} and Cu^{2+} concentrations on gating and conductance of Ca$_v$2.3. To dissociate these two processes, we measured alterations in current amplitudes at −20 and +20 mV, respectively (Fig. 5 A). Changes in the current amplitude measured at +20 largely reflect the effect on conductance, as maximal activation of Ca$_v$2.3 was achieved at about +20 mV (Fig. 2). On the other hand, changes at −20 mV (∼V$_{1/2}$) are primarily associated with the effect on open probability (activation gating), as HEPES to Tricine substitution produced no effect on the channel's permeability. Both cations exerted approximately 10-fold stronger effects on gating than on conductance of Ca$_v$2.3 (Fig. 5, B and C). As a result of this sensitivity

TABLE 2
Free concentrations of Zn^{2+} and Cu^{2+} in 10 mM Tricine

| Zn^{2+}	Added, µM	9.7	100	900		
	Free, µM	0.08	0.8	8		
Cu^{2+}	Added, µM	30	100	269	616	1,100
	Free, nM	13	45	123	293	551

Free concentrations were calculated using the Solver function in the MaxChelator program. Calculations took into account the presence of 1 mM Ca^{2+}, ionic strength (0.15 M), and pH (7.4).
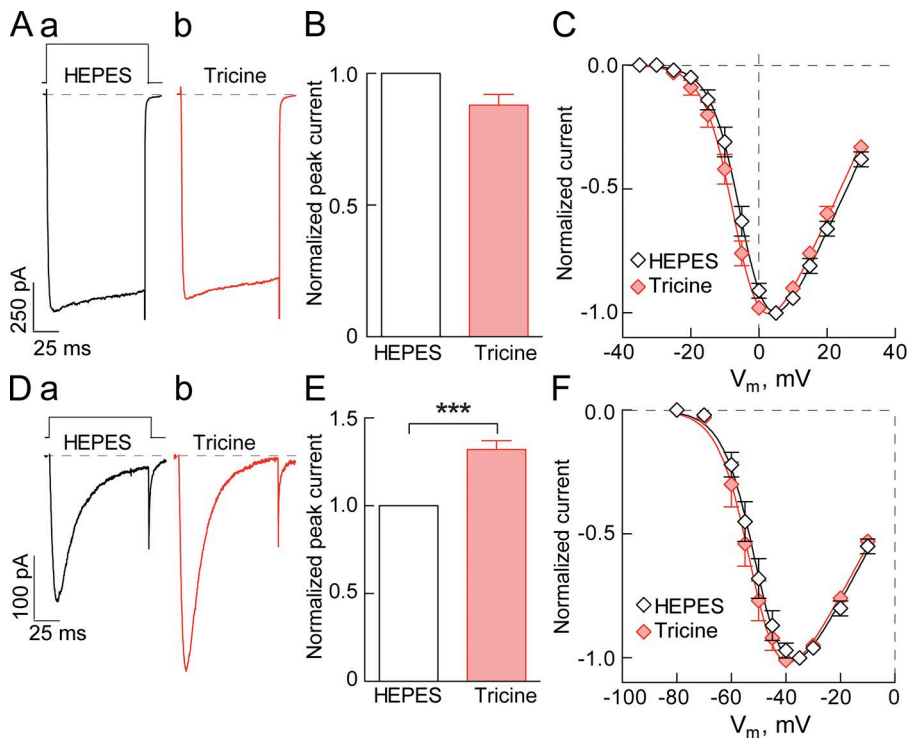
Figure 3. Tricine substitution for HEPES produces no effect on activation gating of $Ca_v2.2$ and $Ca_v3.2$ cannels. (A and D) Representative $Ca_v2.2$ (A) and $Ca_v3.2$ (B) currents recorded at +5 and −30 mV, respectively, in HEPES and Tricine solutions. (B and E) Normalized ratios of peak current amplitudes for $Ca_v2.2$ (B; $n = 6$) and $Ca_v3.2$ (E; $n = 9$) channels. (C and F) Normalized and averaged I-V relationships measured in HEPES and Tricine solutions for $Ca_v2.2$ (C; $n = 6$) and $Ca_v3.2$ (B) channels. Data acquired from each cell were fitted with GHK Eq. 1 ($Ca_v2.2$: HEPES $V_{1/2} = -1.8 \pm 1.0$ and $k = 4.5 \pm 0.2$ mV; Tricine $V_{1/2} = -3.8 \pm 0.9$ and $k = 4.6 \pm 0.2$ mV; $n = 6$; and $Ca_v3.2$: HEPES $V_{1/2} = -47.4 \pm 1.7$ and $k = 6.1 \pm 0.2$ mV; Tricine $V_{1/2} = -48.7 \pm 1.2$ and $k = 6.0 \pm 0.3$ mV; $n = 4$).

pattern, zinc and copper profoundly shifted the voltage dependence of activation of $Ca_v2.3$ toward more positive values (Fig. 5 D and Table 1), also producing a moderate effect on kinetics of inactivation (Table 1) and steady-state inactivation (Fig. 5 E and Table 1). Although gating effects of both trace metals were qualitatively similar, copper was ∼100 times more potent at inhibiting currents at −20 mV than zinc ($IC_{50} = 18.0 \pm 0.4$ nM; $n = 8$ vs. $1,300 \pm 0.4$ nM; $n = 6$; Fig. 5 B). While studying the effects of Zn^{2+} and Cu^{2+} on the current through $Ca_v2.3$ channels (Fig. 6), we also noticed that copper almost completely recapitulated the slow kinetics of current activation/inactivation observed in HEPES solution (Fig. 6, A and C), whereas Zn^{2+} failed to reproduce it at any tested concentration (Fig. 6, B and C).

Finally, we tested the effect of low Cu^{2+} concentration on endogenous residual Ca^{2+} current (R-type; Birnbaumer et al., 1994; Randall and Tsien, 1995), which is believed to be the product of $Ca_v2.3$ channel activity (Schneider et al., 1994; Piedras-Rentería and Tsien, 1998). We recorded IB4-negative (−), medium-sized DRG neurons (Fig. 7 A), which were shown to express SNX-482 sensitive R-type channels (Fang et al., 2007). R-type current was isolated by the bath perfusion of the blocker cocktail until a steady level was achieved (Fig. 7 B), comprising ∼30% of the initial net calcium current measured at +20 mV (Fig. 7 C). Recapitulating the results with the recombinant channel, the application of 45 nM Cu^{2+} shifted the I-V curve of native channels to more depolarized voltages, producing almost no effect on the
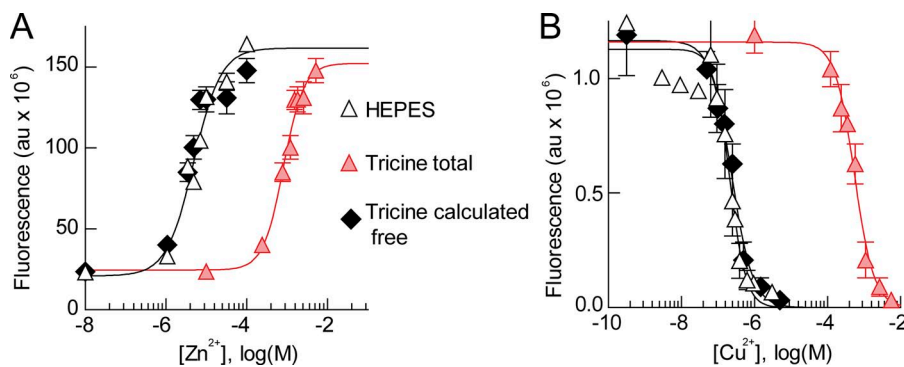
Figure 4. Calibration of free Zn^{2+} and Cu^{2+} concentrations in Tricine solution. (A) Fluorescence from Newport Green DCF (3 µM) was measured after the addition of varying concentrations of $ZnCl_2$ to HEPES- and Tricine-based solutions. HEPES and Tricine solutions used for these experiments only contained 1 mM HEPES and 10 mM Tricine, respectively. KCl was added to adjust the ionic strength to 0.15 M, pH 7.4, KOH. Apparent free concentrations of Zn^{2+} in Tricine solution (Tricine calculated free) were calculated using the Solver function of the MaxChelator program (Patton et al., 2004). (B) Calibration of free Cu^{2+} concentrations in Tricine solution using 3 µM Mag-Fura-2. The addition of $CuCl_2$ led to a dose-dependent quenching of the fluorescent signal. Solver was used to calculate the apparent free concentration of Cu^{2+} in Tricine solution (Tricine calculated free).

amplitude of current measured at positive potentials (Fig. 7, D–F).

Collectively, these results suggest that voltage-dependent gating of Ca$_v$2.3 channels is highly sensitive to trace metals. Copper is a more effective modulator of gating than zinc. Glu and Gly profoundly modulate activity of these channels, acting as trace metal chelators.

Molecular basis of Glu and trace metal sensitivity in Ca$_v$2.3

Inhibition of Ca$_v$3.2 channels by transition metals relies heavily on the histidine (H191) in the IS3–IS4 loop (Kang et al., 2006; Nelson et al., 2007a). Alignment of Ca$_v$2 and Ca$_v$3 channels reveals that Ca$_v$2.3 contains two histidines in the IS3–IS4 loop (H179 and H181), whereas Ca$_v$2.1 and Ca$_v$2.2 do not have any (Fig. 8 A). Additionally, it was shown that corresponding residues are responsible for the effect of Ni^{2+} on Ca$_v$2.3 (Kang et al., 2007). To determine whether these histidines are responsible for the effect of chelators and trace metals on Ca$_v$2.3, we substituted H179 with Glu (H179E), a negatively charged amino acid that resides in the corresponding position of Ca$_v$2.1, and H181 with alanine

(H181A), a neutral amino acid residue (H179E/H181A; Fig. 8 A). As expected from the sequence similarity, the H179E/H181A mutant was completely insensitive to Tricine substitution for HEPES (Fig. 8, B–E). Notably, while in HEPES, H179E/H181A mutants opened in the same voltage range as Ca$_v$2.3 in Tricine solution (Table 1). Additionally, channels with either single–amino acid substitutions were similarly insensitive to 200 µM Gly, 200 µM Glu, or 100 µM DTPA (not depicted). Single mutants were approximately seven times less sensitive to copper (IC$_{50}$ = 142 and 115 nM for H183A and H179E, respectively), whereas channels with double substitution (H179E/H181A) demonstrated around 11-fold lower copper sensitivity (IC$_{50}$ = 203 nM) (Fig. 8 G).

Trace metal–binding amino acids in various ion channels are often scattered along the IS3–IS4 and IS1–IS2 putative extracellular loops (Kang et al., 2006, 2010; Ramsey et al., 2006; Nelson et al., 2007a; Ma et al., 2008). To probe the contribution of His111, residing in the IS1–1S2 loop of Ca$_v$2.3, we substituted it with alanine (H111A; Fig. 8 A). Apparent copper sensitivity again decreased (IC$_{50}$ = 205 nM; Fig. 8 G). Strikingly,
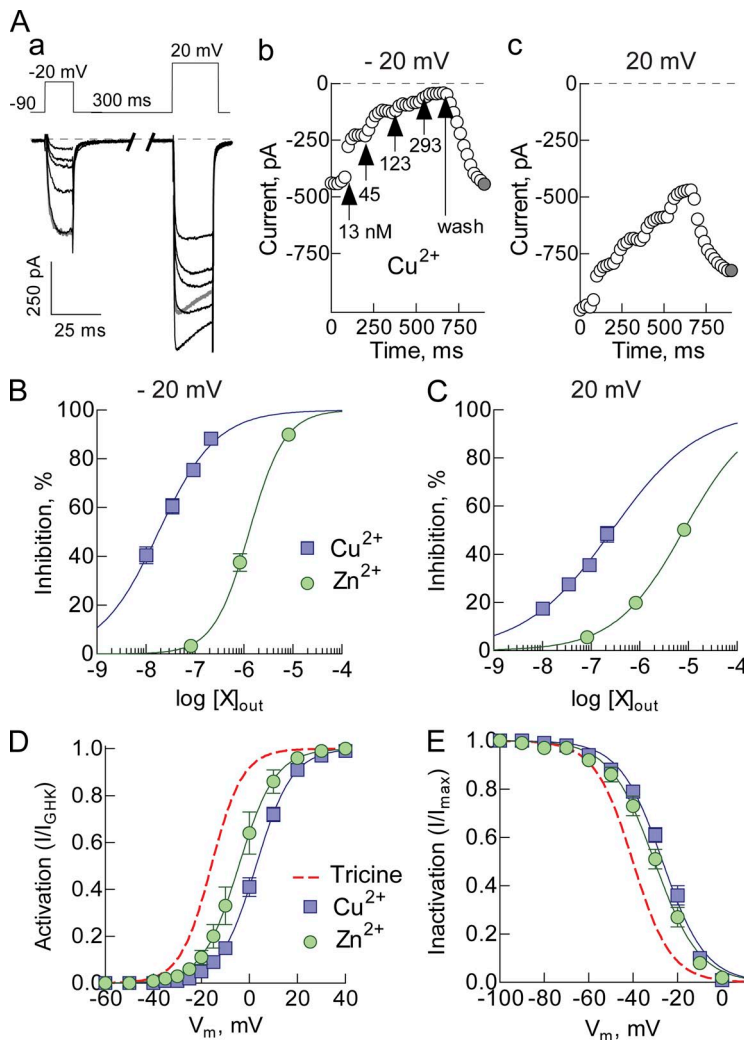

Figure 5. The effects of calibrated Zn^{2+} and Cu^{2+} concentrations on Ca$_v$2.3. (A, a) Representative current traces measured in response to a double-pulse protocol (depicted above) in Tricine- and copper-containing solutions. Copper concentrations at which currents were recorded are indicated in (b). (b and c) Time course of the effect of various Cu^{2+} concentrations on the amplitude of Ca^{2+} currents through Ca$_v$2.3, measured at −20 mV (b) and 20 mV (c). (B) Dose–response curves of the effect of Zn^{2+} and Cu^{2+} on gating of Ca$_v$2.3. Smooth lines represent the fit to the average data with the Hill equation (Zn^{2+}: IC$_{50}$ = 1.3 ± 0.2 µM and n$_H$ = 1.2; n = 6; and Cu^{2+}: IC$_{50}$ = 18.2 ± 3.7 nM and n$_H$ = 0.7; n = 8). (C) Dose–response curves of the effect of Zn^{2+} and Cu^{2+} on conductance of Ca$_v$2.3. Smooth lines represent the fit to the average data with the Hill equation (Zn^{2+}: IC$_{50}$ = 8.1 ± 1.4 µM and n$_H$ = 0.60; n = 6; and Cu^{2+}: IC$_{50}$ = 269 ± 101 nM and n$_H$ = 0.5; n = 8). (D and E) Voltage dependence of activation (D) and steady-state inactivation curves (E), measured in Tricine solution and solutions containing either 8 µM Zn^{2+} or 293 nM Cu^{2+}. Data were fitted with a Boltzmann equation (Table 1).
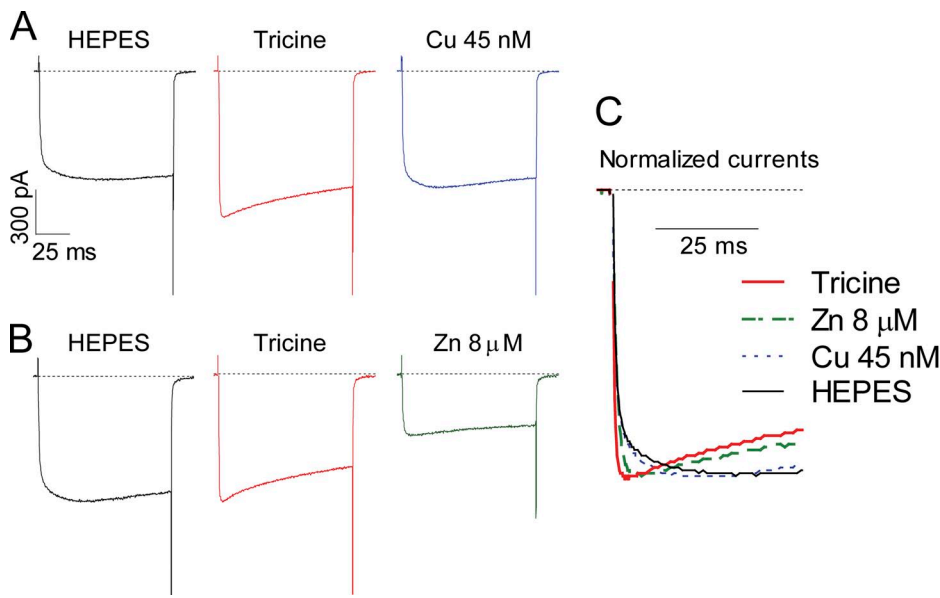
Figure 6. Distinct effects of Cu^{2+} and Zn^{2+} on kinetics of $Ca_v2.3$ currents. (A and B) Representative current recordings obtained in response to a depolarizing pulse to +10 mV (V_{hold} = −90 mV) in HEPES, Tricine, and Cu^{2+}- or Zn^{2+}-containing extracellular solutions. (C) Normalized and averaged current recordings (n = 5).

mutation of all three histidine residues (H111A/H179E/H181A) renders channels practically insensitive to Cu^{2+} (Fig. 8, F–H).

Insights into the biophysical mechanisms of copper action

To gain further insight into the biophysics of copper action on gating of $Ca_v2.3$, we analyzed the time and voltage
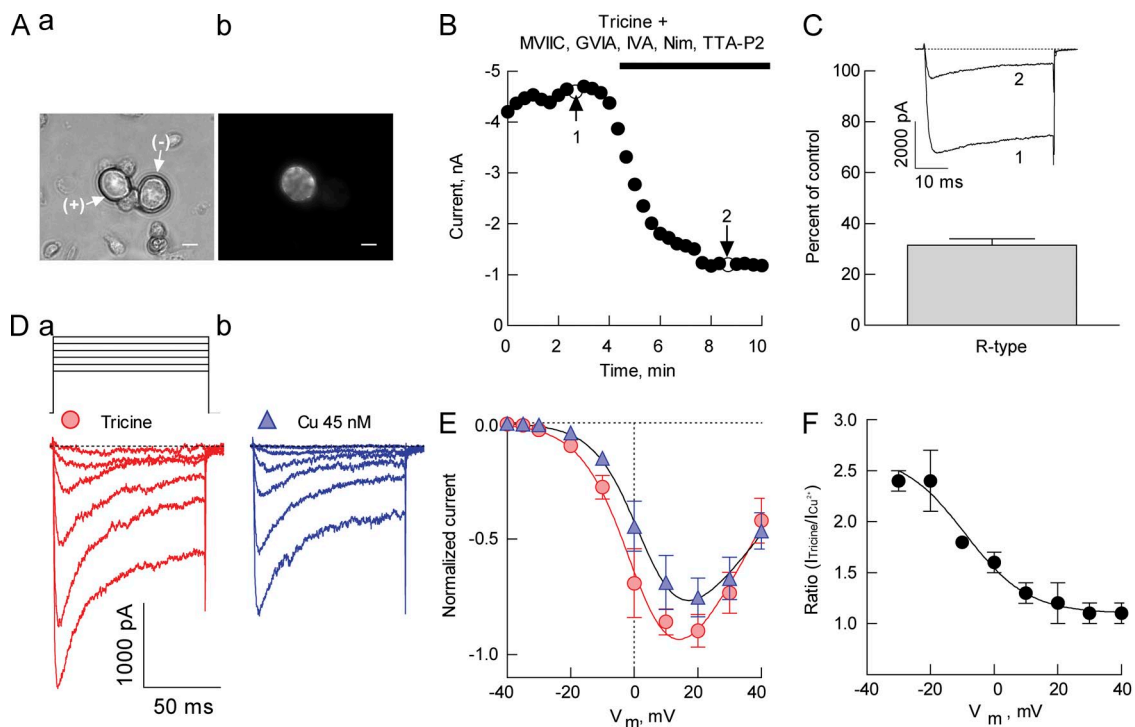

Figure 7. Copper at low concentrations modulates the activation gating of residual (R-type) calcium current in DRG neurons. (A) Bright field and fluorescence images of IB4-positive (+) and IB4-negative (−) DRG neurons, identified by live staining with 10 μg/ml IB4-FITC (Sigma-Aldrich). Bar, 10 μm. (B) Time course of changes in the amplitude of the net Ba^{2+} current through VGCC, recorded from an IB4 (−) neuron in response to a 20-mV voltage step, induced by perfusion of recording chamber with the cocktail of Ca^{2+} channel blockers. (C) In IB4 (−) DRG neurons, ∼30% of the net current at +20 mV is carried through R-type calcium channels (n = 4). (D) Examples of recordings of isolated R-type calcium currents, measured in response to the I-V protocol (V_{hold} = −90 mV, depolarizations to −30, −20, −10, 0, 10, and 20 mV) in Tricine- and Cu^{2+}-containing solutions with 5 mM Ba^{2+} as a charge carrier. (E) Normalized peak current I-V relationships. Data were fit with the standard Boltzmann-Ohm equation (Tricine: $V_{1/2}$ = 3.1 ± 4.9 and k = 6.6 ± 1.3 mV; Cu^{2+}: $V_{1/2}$ = 7.8 ± 3.9* and k = 6.6 ± 1.3 mV; *, P = 0.026 by paired Student's t test; n = 4). (F) The voltage dependence of the Cu^{2+} effect on endogenous R-type current in DRG neurons. The ratio of peak current amplitudes ($I_{Tricine}/I_{Cu}$) at each potential was plotted as a function of potential.

dependence of this process in 13 nM Cu^{2+}, the concentration at which copper exhibited the effect only on activation gating of $Ca_v2.3$ (Fig. 9), but not on mutant channels (Fig. 8 G). At negative voltages, below -15 mV, the effect of copper was relatively time and voltage independent ($\sim$40%); however, it diminished quickly ($\tau = 70$–9 ms) at more depolarized voltages (Fig. 10, A and B). As a result, the effect of Cu^{2+} on $Ca_v2.3$, measured at the peak of current amplitude, was noticeably voltage dependent (Fig. 10 C), counter to the expectation that an extracellular inhibitor should exert a voltage-independent effect.

To test whether the given pattern of Cu^{2+} inhibition arises from intrinsic changes in the activation/inactivation kinetics of the channel or from state-dependent facilitation, akin to the effect of G$\beta\gamma$ subunit on VGCCs

(Elmslie et al., 1990; Boland and Bean, 1993), we tested the effect of a strong depolarizing pulse (+150 mV) on Cu^{2+} inhibition (Fig. 10, D and E). The depolarizing pulse was first delivered in Tricine solution, where it induced an $\sim$10% decrease in current amplitude (T_2 vs. T_1; Fig. 10 D, a). Next, 13 nM Cu^{2+} was added to the extracellular solution and currents were recorded again. In the presence of Cu^{2+}, the +150-mV prepulse completely restored the "fast" kinetics of current activation/inactivation (C_2 vs. C_1; Fig. 10 D, b) and alleviated $\sim$80% of the inhibition induced by Cu^{2+} (Fig. 10 E). These results suggest that Cu^{2+} induces the strongest effect on $Ca_v2.3$ when channels are closed; however, transition into an open state partially relieves this inhibition, producing a prominent slowing effect on the activation/inactivation kinetics.
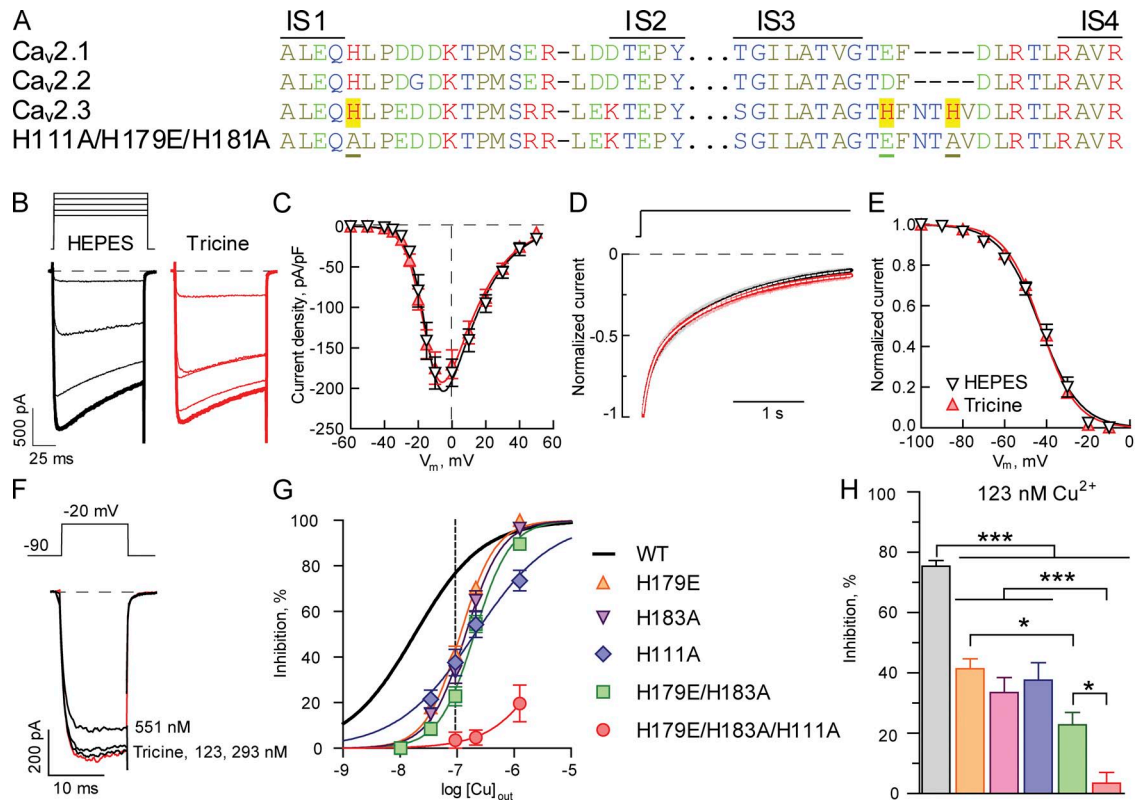

Figure 8. Histidines in the IS1–IS2 and IS3–IS4 loops underlie the trace metal sensitivity of $Ca_v2.3$. (A) Alignment of the putative amino acid residues residing in the IS1–IS2 and IS3–IS4 regions of Ca_v2 channels. Triple histidines, responsible for the trace metal sensitivity in $Ca_v2.3$ (highlighted), were identified by their sequential substitution: H111A/H179E/H181A. (B) Representative current traces recorded from $Ca_v2.3$ channels bearing the H179E/H181A mutation in response to the I-V protocol depicted above ($V_{hold} = -90$ mV, depolarizing pulses from -30 to 10 mV). Highlighted current traces were recorded in response to a -10-mV voltage pulse. (C) Peak current I-V relationships for H179E/H181A mutant obtained in HEPES- or Tricine-based extracellular solutions and normalized to cell capacitance. Data were fitted with GHK Eq. 1 (Table 1). (D) Normalized and averaged Ca^{2+} currents ± SEM (shaded area) recorded in response to prolonged (3-s) depolarizing pulse to -10 mV in HEPES and Tricine solutions. Recordings were fitted with double-exponential function. Corresponding values and statistics are in Table 1. (E) Steady-state inactivation curves for H179E/H181A mutant measured in the HEPES- or Tricine-based extracellular solutions. Data were fitted with a Boltzmann equation (Table 1). (F) Currents through H111A/H179E/H181A mutant channels, measured in response to the voltage pulse depicted above in Tricine- and Cu^{2+}-containing solutions. (G) Dose–response curves of the Cu^{2+} effect on currents through $Ca_v2.3$ channels bearing various point mutations. Smooth lines represent the fit to the average data with the Hill equation (H179E: $IC_{50} = 115 \pm 11$ nM and $n_H = 1.4$; $n = 4$; H183A: $IC_{50} = 142 \pm 19$ nM and $n_H = 1.4$; $n = 4$; H179E/H183A: $IC_{50} = 203 \pm 27$ nM and $n_H = 1.4$; $n = 9$; and H111A: $IC_{50} = 205 \pm 75$ nM and $n_H = 0.6$; $n = 5$). (H) Mean values of inhibition induced by the application of 123 nM Cu^{2+} (***, P < 0.0001; **, P < 0.001; *, P < 0.05 by one-way ANOVA with Bonferroni posthoc correction).
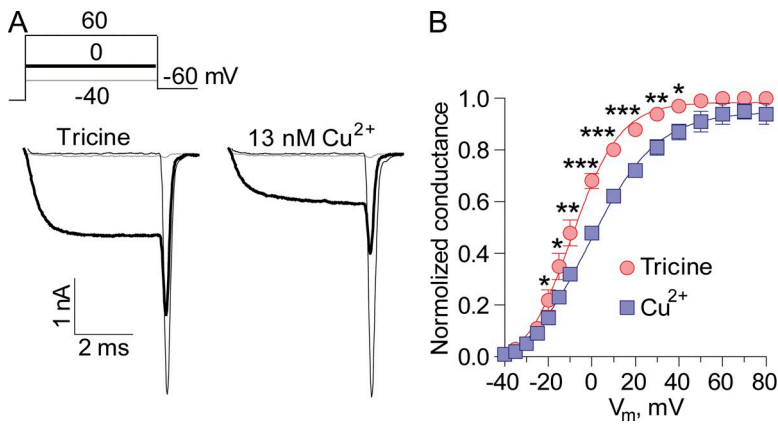
Figure 9. Cu^{2+} at low concentrations produces "pure" effect on the activation gating of $Ca_v2.3$. (A) Tail currents recorded in Tricine- and Cu^{2+}-containing solutions in response to the protocol depicted above. (B) Activation curves obtained from the measurements of the amplitudes of tail currents, normalized to the maximum amplitude of the tail current recorded in Tricine.

Transition of voltage-gated channels between the closed and open states is associated with significant perturbations in voltage-sensor domains (S1–S4), manifested as gating current in electrophysiological experiments (Swartz, 2008). In K^+ channels, it was shown that S1–S2 and S3–S4 loops are close to each other in the closed conformation, but move apart upon channel opening (Campos et al., 2007). Therefore, we tested whether Cu^{2+} produces its effects on $Ca_v2.3$ by affecting gating charge movement. We measured gating current in response to depolarization to the reversal membrane potentials (57 ± 2 mV; $n = 7$) (Fig. 11 A). Interestingly, the total gating charge displacement across the membrane field stayed the same (Fig. 11 B); however, the amplitude of the gating current and its decay time were significantly different (Fig. 11, C and D). Thus, in Tricine solution, the amplitude was significantly greater (490 ± 98 vs. 440 ± 87 pA), but the kinetics of decay was faster (0.13 ± 0.02 vs. 0.17 ± 0.03 ms). Accordingly, the Cu^{2+}-induced positive shift in voltage dependence of $Ca_v2.3$
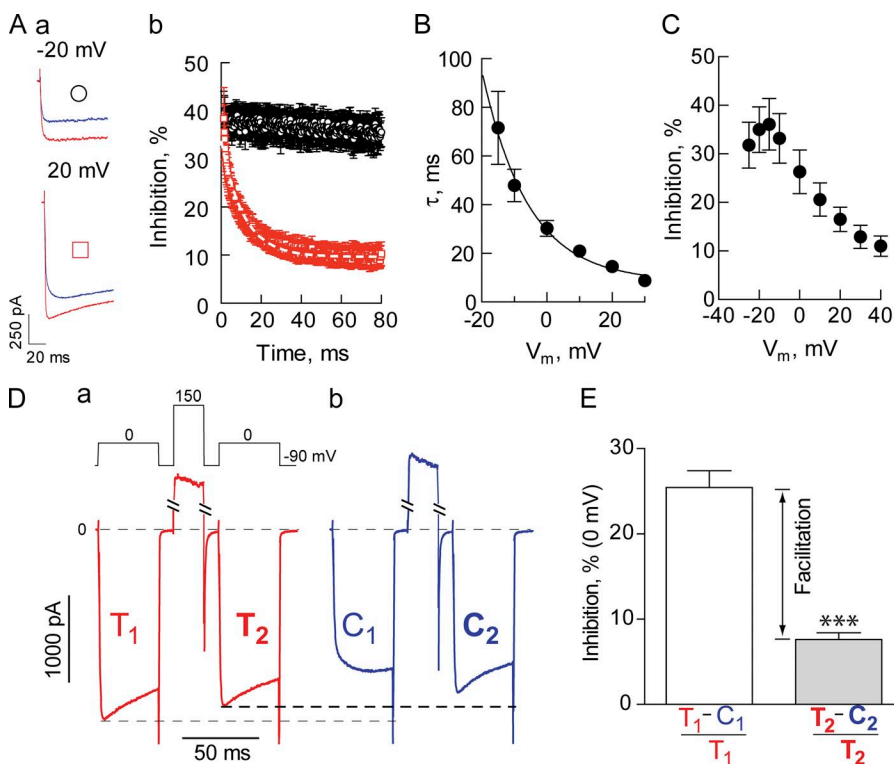
Figure 10. Cu^{2+} affects gating of $Ca_v2.3$ through the extracellular binding site in a state-dependent manner. (A) Time dependence of the inhibitory effect of 13 nM Cu^{2+} on currents through $Ca_v2.3$ channels, induced by depolarization to -20 or 20 mV (a). The percentage of inhibition at each time point was calculated as a difference in current amplitudes measured in Tricine (black traces) and Cu^{2+} solutions (gray traces), divided by the amplitude in Tricine (b). (B) Voltage dependence of the kinetics of facilitation of Cu^{2+} inhibition. Time constants were determined from A by fitting time dependences with the monoexponential functions ($n = 6$). (C) Voltage dependence of the inhibition of current through $Ca_v2.3$ channels by 13 nM Cu^{2+}. The percentage of inhibition at each voltage was calculated as a difference between peak current amplitudes measured in Tricine and Cu^{2+} solutions divided by the current amplitude in Tricine ($n = 6$). (D) Strong depolarization partially reverses the inhibitory effect of Cu^{2+} on $Ca_v2.3$. Current traces were recorded in response to the protocol depicted above in Tricine- (a) and Cu^{2+}-containing (b) solutions (13 nM). (E) Quantification of the Cu^{2+} inhibition of $Ca_v2.3$ current, recorded before ((T_1–C_1)/T_1) or after ((T_2–C_2)/T_2) the delivery of a depolarizing pulse to 150 mV ($n = 5$; ***, $P < 0.0001$ with paired Student's t test).

could emerge as a result of slower "ON" transitions of gating charges and a decreased fraction of channels open at a given potential.

DISCUSSION

We show that neurotransmitters such as Glu and Gly and trace metals such as Zn^{2+} and Cu^{2+} profoundly modulate activity of $Ca_v2.3$ calcium channels by influencing their voltage-dependent gating. We identified a trace metal–binding site on the extracellular surface of the channel and demonstrated that, once bound there, trace metals decelerate the transition of gating charges into the "ON" position in response to membrane depolarization. This finding provides a new perspective on the role played by Glu and trace metals, both present within the synaptic clefts of many excitatory synapses, in synaptic transmission and plasticity.

Glu as a potent agonist for $Ca_v2.3$

Glu and its targets in the brain have been the subject of extensive investigation since their discovery. Once released from the presynaptic terminal, Glu rapidly finds its receptors on the pre-/postsynaptic membranes, conveying information between interconnected neurons. Glu concentration, its spatiotemporal profile, and the identity of the targets of the neurotransmitter are all of high importance for proper signal transduction in the brain. Here, we identified $Ca_v2.3$ channels as a new target for Glu. Glu substantially potentiated activity of these channels at hyperpolarized potentials by shifting their voltage-dependent activation curve toward more negative voltages (Fig. 1). Remarkably, the effect of Glu on $Ca_v2.3$ is mechanistically distinct from that reported previously (Stea et al., 1995), as this modulation does not rely on the recruitment of any intracellular cascades. Instead, Glu exerts its action on $Ca_v2.3$ from the extracellular side, by acting as a trace metal chelator. Although the ability of Glu to bind trace metals is well documented (Dawson et al., 1986), this role has mostly been neglected in the context of physiological experiments. Given that local transient concentration of Glu in the synaptic cleft can reach the millimolar range (Clements et al., 1992), all Glu-sensitive postsynaptic channels and receptors should be considered as potential targets. However, in contrast with Glu receptors, the sensitivity of $Ca_v2.3$ to Glu relies on the presence of trace metals in the extracellular milieu. Notably, the concentration of free or loosely bound Zn^{2+} and Cu^{2+} is elevated in the brain (Osterberg, 1980; Mathie et al., 2006), and the release of these metals from synaptic vesicles in a voltage- and Ca^{2+}-dependent fashion has been detected with various techniques (Assaf and Chung, 1984; Howell et al., 1984; Hartter and Barnea, 1988; Kardos et al., 1989; Hopt et al., 2003; Frederickson et al., 2005).

The trace metal hypersensitivity of $Ca_v2.3$

The effect of transition metals, mostly zinc, on the activity of VGCCs was investigated previously in several studies (Nam and Hockberger, 1992; Büsselberg et al., 1994; Easaw et al., 1999; Castelli et al., 2003; Magistretti et al., 2003; Sun et al., 2007). It was shown that R-type calcium channels in cortical neurons are sensitive to micromolar
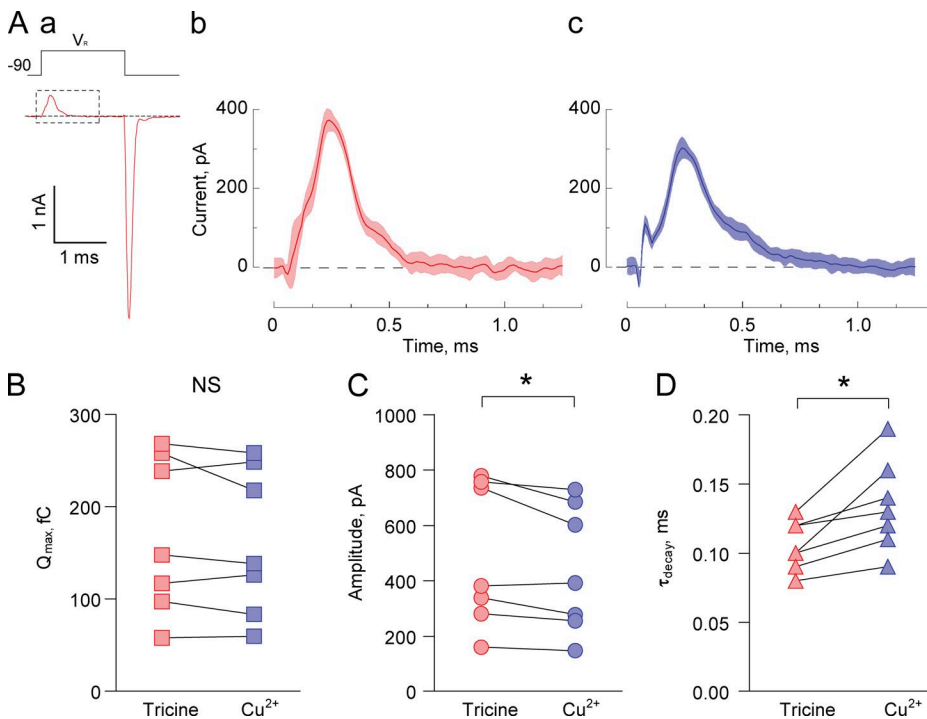
Figure 11. A low concentration of Cu^{2+} (13 nM) decelerates gating charge movement in $Ca_v2.3$. (A) Representative gating current traces (the average of 20 consecutive runs ± SD) recorded in response to the step depolarization to the reversal potential ($V_r = 58 ± 2$ mV; $n = 8$) in Tricine- (a and b) and Cu^{2+}-containing (c) solutions (13 nM). (b and c) Enlarged view of the region selected with dashed lines on (a). (B) Maximal gating charges transferred across membrane in Tricine- and Cu^{2+}-containing solutions ($n = 7$). (C) Amplitudes of the gating current transients recorded in Tricine- and Cu^{2+}-containing solutions (*, $P = 0.043$, by paired Student's t test; $n = 7$). (D) Time constants of the gating current transient decay measured in Tricine and Cu^{2+} solutions (*, $P = 0.014$, by paired Student's t test; $n = 7$).

concentrations of copper and zinc, which allosterically modulate the activation/deactivation kinetics of the channel (Castelli et al., 2003; Magistretti et al., 2003). Additionally, it was demonstrated that Ni^{2+} at a micromolar concentration inhibits $Ca_v2.3$ by shifting its gating to more depolarized voltages (Zamponi et al., 1996), and that the Ni^{2+}-binding site also contains H179 and H181 at its core (Kang et al., 2007). Although $Ca_v2.3$ current that activates at relatively depolarized voltages and possesses relatively slow activation/inactivation kinetics has also been observed previously (Page et al., 1998; Jouvenceau et al., 2000), it has never before been reported that the trace amounts of metals that often contaminate extracellular solutions (Kay, 2004) exert a tonic inhibitory effect on $Ca_v2.3$ voltage-dependent gating. Based on the positions of I-V curve and current kinetics in the presence of various Zn^{2+} and Cu^{2+} concentrations (Fig. 6), we estimated that our HEPES–TEA solution contains ∼50 nM Cu^{2+}, which is responsible for the 17-mV negative shift in the activation curve observed upon substitution of HEPES for Tricine. Interestingly, this substitution also accelerated current inactivation kinetics (Fig. 2 E). These effects are similar to what was previously observed after the removal of Gβγ inhibition of Ca_v2 channels (Tedford and Zamponi, 2006). Thus, they might also be a consequence of the slowed activation gating induced by trace metals, as Gβγ activity was suppressed by the presence of $GDPβ_S$ in the internal solution.

Various ion channels including Glu, Gly, $GABA_A$, acetylcholine, P2X receptors, and Na^+ ($Na_v1.5$), K^+ (K2P, $K_v1.3$, mSlo1), and Ca^{2+} ($Ca_v3.2$) channels (Mathie et al., 2006; Traboulsie et al., 2007; Ma et al., 2008) were reported to be sensitive toward zinc and copper at concentrations below 10 μM. However, only NMDA receptors and $Ca_v3.2$ calcium channels could be tonically blocked by trace amounts of zinc (Paoletti et al., 1997;

Nelson et al., 2007b). Our study identifies $Ca_v2.3$ as the most sensitive target of copper among other channels and receptors (NMDAR: IC_{50} = 270 nM [Vlachová et al., 1996]; $Ca_v3.2$: IC_{50} = 900 nM [Jeong et al., 2003]). To reveal this trace metal hypersensitivity, we followed the approach originally proposed by Paoletti et al. (1997) and used Tricine to chelate contaminating trace metals in our extracellular solution. Furthermore, we used fluorescent dyes to calibrate free concentrations of Zn^{2+} and Cu^{2+} in the Tricine solution. Thus, we discovered that relatively low concentrations of Zn^{2+} and Cu^{2+} (IC_{50} = 1,300 and 18 nM, respectively) profoundly modulate the activity of $Ca_v2.3$.

Putative mechanism of copper interaction with $Ca_v2.3$

To describe the molecular mechanism likely responsible for copper modulation of $Ca_v2.3$ gating, we produced a model (Fig. 12) that summarizes our results in the context of what is known about the open and closed conformations of voltage-gated channels in general (Swartz, 2008). In a closed conformation, the top portions of the S4 and S1–S2 segments reside in close proximity to each other (Chanda et al., 2005; Campos et al., 2007), such that H111, H179, and H183 residues form a high affinity binding site for trace metals (Fig. 12 A). However, changes in the electric field can induce a translocation of S4 into a second position (Long et al., 2007) and break this binding pocket (Fig. 12 B). Remarkably, a high affinity binding site for trace metals consisting of three histidines is found in a variety of natural proteins and can be artificially introduced into a four-helix bundle protein, by placing two histidines on one helix as His–X_3–His and the third on an adjacent helix (Regan, 1993). Thus, trace metals bind to the IS1–IS4 gating module of $Ca_v2.3$ in a state-dependent manner and, once bound, decelerate "ON" transitions of gating charges. This modulatory action should decrease
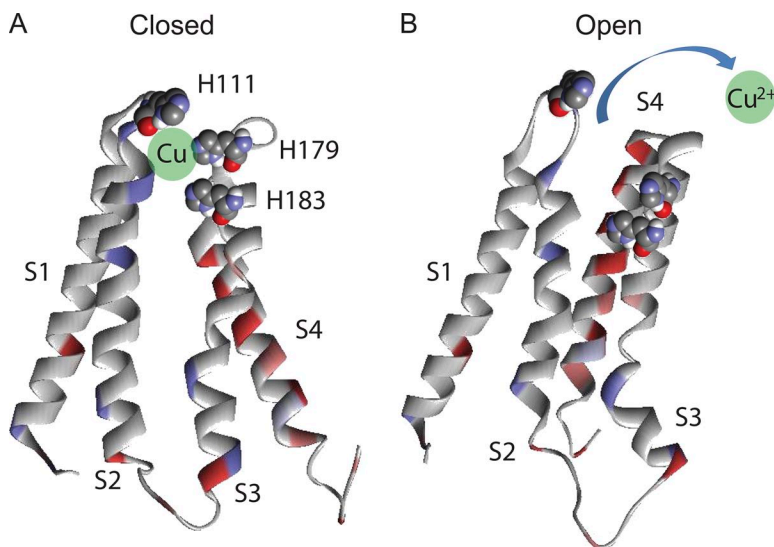
Figure 12. Putative model of Cu^{2+} interaction with the gating machinery of $Ca_v2.3$. Residues responsible for Cu^{2+} binding in $Ca_v2.3$ (H111, H179, and H183) were mapped onto the structural model of a voltage-gated potassium channel (Chanda et al., 2005; Campos et al., 2007). Only the S1–S4 segments from the first domain are shown. (A) In closed conformation, histidines of IS1–IS2 and IS3–IS4 loops of $Ca_v2.3$ are situated close to each other and can bind Cu^{2+} if it is present in the solution. The green sphere illustrates a possible position for Cu^{2+}. (B) Upon channel opening, histidines are moved apart by the gating machinery, which apparently disrupts the binding pocket and releases Cu^{2+} from the binding site.

the fraction of channels open at a given potential, inducing a positive shift of voltage dependence and slowing the activation kinetics of the current.

Our hypothetical model is supported by the following observations. First, trace metals selectively modulate voltage-dependent gating of $Ca_v2.3$, inducing almost no effect on conductance (Table 1). Second, key amino acid residues (H111, H179, and H183) responsible for trace metal binding in $Ca_v2.3$ reside within the gating module on the extracellular side of the channel (Fig. 8). Third, a high level of inhibition by trace metals was detected for channels in the closed state, whereas a reduction in inhibition was seen upon activation/inactivation (Fig. 10, A–C). Fourth, a significant percentage of inhibition was reversed by a strong depolarizing prepulse, which brings voltage sensors into an open-state position (Fig. 10, D and E). Finally, copper decelerates the transition of gating charges into the "ON" state, rendering the total charge translocation unaffected (Fig. 11).

The presence of a trace metal–binding site within a gating module seems to be a common feature of various voltage-gated channels, including Hv1 (Ramsey et al., 2006), Cav3.2 (Kang et al., 2006; Nelson et al., 2007a), and Slo1 (Ma et al., 2008). Whereas in Hv1 and Cav3.2 His has also been identified at the core of the trace metal–binding site, in Slo1 channels, a copper-binding site with lower affinity (2 µM) is formed by charged amino acid residues. This suggests a common conservative conformation of the closed state across the family of voltage-gated channels.

Physiological implication

Although $Ca_v2.3$ channels are implicated in several vital physiological processes, arguably the most prominent roles attributed to these channels are to trigger presynaptic LTP at mossy fiber–CA3 synapses (Breustedt et al., 2003; Dietrich et al., 2003) and to regulate membrane depolarization and Ca^{2+} influx in the dendritic spines of CA1 pyramidal neurons (Bloodgood and Sabatini, 2007). LTP at mossy fiber synapses is thought to rely mostly on presynaptic changes after tetanic stimulation (Nicoll and Schmitz, 2005). Two studies have revealed the critical involvement of presynaptic $Ca_v2.3$ calcium channels in the induction, but not expression, of this form of synaptic plasticity (Breustedt et al., 2003; Dietrich et al., 2003). Notably, it was shown that Ca^{2+} influx through these channels substantially increases in response to AP series, whereas the application of 100 µM Ni^{2+} depresses LTP induction. Based on our findings, we can speculate that Glu released during tetanic stimulation acts as a chelator on presynaptic $Ca_v2.3$ channels, abrogating their tonic inhibition by trace metals and thereby potentiating Ca^{2+} entry into the mossy fiber terminal through these channels.

R-type calcium channels on the dendritic spines of CA1 pyramidal neurons are involved in a negative feedback loop that regulates NMDAR activity (Bloodgood and Sabatini, 2007; Giessel and Sabatini, 2010). It was shown that these channels can be activated not only in response to back-propagating AP but also upon stimulation of a single spine with uncaged Glu. R-type channels consequently provide an important route for Ca^{2+} entrance into the spine, reducing the amplitude of EPSP and depressing NMDAR activity. Nevertheless, it is unclear how R-type Ca^{2+} channels can be activated by a single transient EPSC with average amplitude of <1 mV measured at the soma. Our findings provide a possible answer for this question. Taking into consideration the high concentration of Glu in the synaptic cleft, we suggest that Glu chelation of trace metals shifts the activation of $Ca_v2.3$ channels sufficiently to allow them to open in response to a small membrane depolarization.

Author contributions: A. Shcheglovitov and E. Perez-Reyes generated the hypotheses and designed the experiments. A. Shcheglovitov performed experiments for all figures and analyzed the data. E. Perez-Reyes generated data in Figs. 4 and 12. R.M. Lazarenko generated data in Figs. 8 and 11 and commented on the manuscript, and I. Vitko generated data in Fig. 8. P. Orestes prepared DRG neurons for experiments shown in Fig. 7. S.M. Todorovic provided reagents and commented on the manuscript. A. Shcheglovitov and E. Perez-Reyes wrote the paper.

REFERENCES

Aslamkhan, A.G., A. Aslamkhan, and G.A. Ahearn. 2002. Preparation of metal ion buffers for biological experimentation: a methods approach with emphasis on iron and zinc. *J. Exp. Zool.* 292:507–522. http://dx.doi.org/10.1002/jez.10068

Assaf, S.Y., and S.H. Chung. 1984. Release of endogenous Zn^{2+} from brain tissue during activity. *Nature.* 308:734–736. http://dx.doi.org/10.1038/308734a0

Bannister, R.A., K. Melliti, and B.A. Adams. 2004. Differential modulation of $Ca_v2.3$ Ca^{2+} channels by Gαq/11-coupled muscarinic receptors. *Mol. Pharmacol.* 65:381–388. http://dx.doi.org/10.1124/mol.65.2.381

Barnham, K.J., and A.I. Bush. 2008. Metals in Alzheimer's and Parkinson's diseases. *Curr. Opin. Chem. Biol.* 12:222–228. http://dx.doi.org/10.1016/j.cbpa.2008.02.019

Birnbaumer, L., K.P. Campbell, W.A. Catterall, M.M. Harpold, F. Hofmann, W.A. Horne, Y. Mori, A. Schwartz, T.P. Snutch, T. Tanabe,

et al. 1994. The naming of voltage-gated calcium channels. *Neuron.* 13:505–506. http://dx.doi.org/10.1016/0896-6273(94)90021-3

Bloodgood, B.L., and B.L. Sabatini. 2007. Nonlinear regulation of unitary synaptic signals by CaV(2.3) voltage-sensitive calcium channels located in dendritic spines. *Neuron.* 53:249–260. http://dx.doi.org/10.1016/j.neuron.2006.12.017

Boland, L.M., and B.P. Bean. 1993. Modulation of N-type calcium channels in bullfrog sympathetic neurons by luteinizing hormone-releasing hormone: kinetics and voltage dependence. *J. Neurosci.* 13:516–533.

Breustedt, J., K.E. Vogt, R.J. Miller, R.A. Nicoll, and D. Schmitz. 2003. α_{1E}-Containing Ca^{2+} channels are involved in synaptic plasticity. *Proc. Natl. Acad. Sci. USA.* 100:12450–12455. http://dx.doi.org/10.1073/pnas.2035117100

Büsselberg, D., B. Platt, D. Michael, D.O. Carpenter, and H.L. Haas. 1994. Mammalian voltage-activated calcium channel currents are blocked by Pb2+, Zn2+, and Al3+. *J. Neurophysiol.* 71:1491–1497.

Campos, F.V., B. Chanda, B. Roux, and F. Bezanilla. 2007. Two atomic constraints unambiguously position the S4 segment relative to S1 and S2 segments in the closed state of Shaker K channel. *Proc. Natl. Acad. Sci. USA.* 104:7904–7909. http://dx.doi.org/10.1073/pnas.0702638104

Castelli, L., F. Tanzi, V. Taglietti, and J. Magistretti. 2003. Cu2+, Co2+, and Mn2+ modify the gating kinetics of high-voltage-activated Ca2+ channels in rat palaeocortical neurons. *J. Membr. Biol.* 195:121–136. http://dx.doi.org/10.1007/s00232-003-0614-2

Catterall, W.A., E. Perez-Reyes, T.P. Snutch, and J. Striessnig. 2005. International Union of Pharmacology. XLVIII. Nomenclature and structure-function relationships of voltage-gated calcium channels. *Pharmacol. Rev.* 57:411–425. http://dx.doi.org/10.1124/pr.57.4.5

Chanda, B., O.K. Asamoah, R. Blunck, B. Roux, and F. Bezanilla. 2005. Gating charge displacement in voltage-gated ion channels involves limited transmembrane movement. *Nature.* 436:852–856. http://dx.doi.org/10.1038/nature03888

Clapham, D.E. 2007. Calcium signaling. *Cell.* 131:1047–1058. http://dx.doi.org/10.1016/j.cell.2007.11.028

Clements, J.D., R.A. Lester, G. Tong, C.E. Jahr, and G.L. Westbrook. 1992. The time course of glutamate in the synaptic cleft. *Science.* 258:1498–1501. http://dx.doi.org/10.1126/science.1359647

Dawson, R.M.C., D.C. Elliott, W.H. Elliott, and K.M. Jones. 1986. Data for Biochemical Research. Third edition. Oxford Science, New York. 592 pp.

Dietrich, D., T. Kirschstein, M. Kukley, A. Pereverzev, C. von der Brelie, T. Schneider, and H. Beck. 2003. Functional specialization of presynaptic Cav2.3 Ca2+ channels. *Neuron.* 39:483–496. http://dx.doi.org/10.1016/S0896-6273(03)00430-6

Easaw, J.C., B.S. Jassar, K.H. Harris, and J.H. Jhamandas. 1999. Zinc modulation of ionic currents in the horizontal limb of the diagonal band of Broca. *Neuroscience.* 94:785–795. http://dx.doi.org/10.1016/S0306-4522(99)00308-5

Ellinor, P.T., J.-F. Zhang, A.D. Randall, M. Zhou, T.L. Schwarz, R.W. Tsien, and W.A. Horne. 1993. Functional expression of a rapidly inactivating neuronal calcium channel. *Nature.* 363:455–458. http://dx.doi.org/10.1038/363455a0

Elmslie, K.S., W. Zhou, and S.W. Jones. 1990. LHRH and GTP-gamma-S modify calcium current activation in bullfrog sympathetic neurons. *Neuron.* 5:75–80. http://dx.doi.org/10.1016/0896-6273(90)90035-E

Fang, Z., C.K. Park, H.Y. Li, H.Y. Kim, S.H. Park, S.J. Jung, J.S. Kim, A. Monteil, S.B. Oh, and R.J. Miller. 2007. Molecular basis of Ca(v)2.3 calcium channels in rat nociceptive neurons. *J. Biol. Chem.* 282:4757–4764. http://dx.doi.org/10.1074/jbc.M605248200

Frederickson, C.J., J.Y. Koh, and A.I. Bush. 2005. The neurobiology of zinc in health and disease. *Nat. Rev. Neurosci.* 6:449–462. http://dx.doi.org/10.1038/nrn1671

Gasparini, S., A.M. Kasyanov, D. Pietrobon, L.L. Voronin, and E. Cherubini. 2001. Presynaptic R-type calcium channels contribute to fast excitatory synaptic transmission in the rat hippocampus. *J. Neurosci.* 21:8715–8721.

Giessel, A.J., and B.L. Sabatini. 2010. M1 muscarinic receptors boost synaptic potentials and calcium influx in dendritic spines by inhibiting postsynaptic SK channels. *Neuron.* 68:936–947. http://dx.doi.org/10.1016/j.neuron.2010.09.004

Hartter, D.E., and A. Barnea. 1988. Evidence for release of copper in the brain: depolarization-induced release of newly taken-up 67copper. *Synapse.* 2:412–415. http://dx.doi.org/10.1002/syn.890020408

Haugland, P.R. 2005. The Handbook—A Guide to Fluorescent Probes and Labeling Technologies. 10th edition. Invitrogen, Carlsbad, CA. 1126 pp.

Hopt, A., S. Korte, H. Fink, U. Panne, R. Niessner, R. Jahn, H. Kretzschmar, and J. Herms. 2003. Methods for studying synaptosomal copper release. *J. Neurosci. Methods.* 128:159–172. http://dx.doi.org/10.1016/S0165-0270(03)00173-0

Hosie, A.M., E.L. Dunne, R.J. Harvey, and T.G. Smart. 2003. Zinc-mediated inhibition of GABA(A) receptors: discrete binding sites underlie subtype specificity. *Nat. Neurosci.* 6:362–369. http://dx.doi.org/10.1038/nn1030

Howell, G.A., M.G. Welch, and C.J. Frederickson. 1984. Stimulation-induced uptake and release of zinc in hippocampal slices. *Nature.* 308:736–738. http://dx.doi.org/10.1038/308736a0

Jeong, S.W., B.G. Park, J.Y. Park, J.W. Lee, and J.H. Lee. 2003. Divalent metals differentially block cloned T-type calcium channels. *Neuroreport.* 14:1537–1540. http://dx.doi.org/10.1097/00001756-200308060-00028

Jouvenceau, A., F. Giovannini, C.P. Bath, E. Trotman, and E. Sher. 2000. Inactivation properties of human recombinant class E calcium channels. *J. Neurophysiol.* 83:671–684.

Kamatchi, G.L., R. Franke, C. Lynch III, and J.J. Sando. 2004. Identification of sites responsible for potentiation of type 2.3 calcium currents by acetyl-beta-methylcholine. *J. Biol. Chem.* 279:4102–4109. http://dx.doi.org/10.1074/jbc.M308606200

Kang, H.-W., J.-Y. Park, S.-W. Jeong, J.-A. Kim, H.-J. Moon, E. Perez-Reyes, and J.-H. Lee. 2006. A molecular determinant of nickel inhibition in $Ca_v3.2$ T-type calcium channels. *J. Biol. Chem.* 281:4823–4830. http://dx.doi.org/10.1074/jbc.M510197200

Kang, H.W., H.J. Moon, S.H. Joo, and J.H. Lee. 2007. Histidine residues in the IS3-IS4 loop are critical for nickel-sensitive inhibition of the Cav2.3 calcium channel. *FEBS Lett.* 581:5774–5780. http://dx.doi.org/10.1016/j.febslet.2007.11.045

Kang, H.W., I. Vitko, S.S. Lee, E. Perez-Reyes, and J.H. Lee. 2010. Structural determinants of the high affinity extracellular zinc binding site on Cav3.2 T-type calcium channels. *J. Biol. Chem.* 285:3271–3281. http://dx.doi.org/10.1074/jbc.M109.067660

Kardos, J., I. Kovács, F. Hajós, M. Kálmán, and M. Simonyi. 1989. Nerve endings from rat brain tissue release copper upon depolarization. A possible role in regulating neuronal excitability. *Neurosci. Lett.* 103:139–144. http://dx.doi.org/10.1016/0304-3940(89)90565-X

Karlin, K.D. 1993. Metalloenzymes, structural motifs, and inorganic models. *Science.* 261:701–708. http://dx.doi.org/10.1126/science.7688141

Kay, A.R. 2004. Detecting and minimizing zinc contamination in physiological solutions. *BMC Physiol.* 4:4. http://dx.doi.org/10.1186/1472-6793-4-4

Kuzmiski, J.B., W. Barr, G.W. Zamponi, and B.A. MacVicar. 2005. Topiramate inhibits the initiation of plateau potentials in CA1 neurons by depressing R-type calcium channels. *Epilepsia.* 46:481–489. http://dx.doi.org/10.1111/j.0013-9580.2005.35304.x

Long, S.B., X. Tao, E.B. Campbell, and R. MacKinnon. 2007. Atomic structure of a voltage-dependent K+ channel in a lipid

membrane-like environment. *Nature.* 450:376–382. http://dx.doi
.org/10.1038/nature06265

Ma, Z., K.Y. Wong, and F.T. Horrigan. 2008. An extracellular
Cu^{2+} binding site in the voltage sensor of BK and Shaker potassium channels. *J. Gen. Physiol.* 131:483–502. http://dx.doi.org/
10.1085/jgp.200809980

Magistretti, J., L. Castelli, V. Taglietti, and F. Tanzi. 2003. Dual effect
of Zn2+ on multiple types of voltage-dependent Ca2+ currents
in rat palaeocortical neurons. *Neuroscience.* 117:249–264. http://
dx.doi.org/10.1016/S0306-4522(02)00865-5

Mathie, A., G.L. Sutton, C.E. Clarke, and E.L. Veale. 2006. Zinc and
copper: pharmacological probes and endogenous modulators
of neuronal excitability. *Pharmacol. Ther.* 111:567–583. http://
dx.doi.org/10.1016/j.pharmthera.2005.11.004

Metz, A.E., T. Jarsky, M. Martina, and N. Spruston. 2005. R-type calcium channels contribute to afterdepolarization and bursting in
hippocampal CA1 pyramidal neurons. *J. Neurosci.* 25:5763–5773.
http://dx.doi.org/10.1523/JNEUROSCI.0624-05.2005

Nam, S.C., and P.E. Hockberger. 1992. Divalent ions released from
stainless steel hypodermic needles reduce neuronal calcium
currents. *Pflugers Arch.* 420:106–108. http://dx.doi.org/10.1007/
BF00378649

Nelson, M.T., P.M. Joksovic, E. Perez-Reyes, and S.M. Todorovic.
2005. The endogenous redox agent L-cysteine induces T-type
Ca^{2+} channel-dependent sensitization of a novel subpopulation
of rat peripheral nociceptors. *J. Neurosci.* 25:8766–8775. http://
dx.doi.org/10.1523/JNEUROSCI.2527-05.2005

Nelson, M.T., P.M. Joksovic, P. Su, H.W. Kang, A. Van Deusen, J.P.
Baumgart, L.S. David, T.P. Snutch, P.Q. Barrett, J.H. Lee, et al.
2007a. Molecular mechanisms of subtype-specific inhibition
of neuronal T-type calcium channels by ascorbate. *J. Neurosci.*
27:12577–12583. http://dx.doi.org/10.1523/JNEUROSCI.2206-
07.2007

Nelson, M.T., J. Woo, H.-W. Kang, I. Vitko, P.Q. Barrett, E. Perez-
Reyes, J.-H. Lee, H.-S. Shin, and S.M. Todorovic. 2007b. Reducing
agents sensitize C-type nociceptors by relieving high-affinity zinc
inhibition of T-type calcium channels. *J. Neurosci.* 27:8250–8260.
http://dx.doi.org/10.1523/JNEUROSCI.1800-07.2007

Nicoll, R.A., and D. Schmitz. 2005. Synaptic plasticity at hippocampal mossy fibre synapses. *Nat. Rev. Neurosci.* 6:863–876. http://
dx.doi.org/10.1038/nrn1786

Osterberg, R. 1980. Physiology and pharmacology of copper.
Pharmacol. Ther. 9:121–146. http://dx.doi.org/10.1016/0163-7258
(80)90019-4

Page, K.M., C. Cantí, G.J. Stephens, N.S. Berrow, and A.C.
Dolphin. 1998. Identification of the amino terminus of neuronal Ca2+ channel alpha1 subunits alpha1B and alpha1E as an
essential determinant of G-protein modulation. *J. Neurosci.* 18:
4815–4824.

Paoletti, P., P. Ascher, and J. Neyton. 1997. High-affinity zinc inhibition of NMDA NR1-NR2A receptors. *J. Neurosci.* 17:5711–5725.

Paoletti, P., A.M. Vergnano, B. Barbour, and M. Casado. 2009. Zinc
at glutamatergic synapses. *Neuroscience.* 158:126–136. http://
dx.doi.org/10.1016/j.neuroscience.2008.01.061

Park, J.Y., S. Remy, J. Varela, D.C. Cooper, S. Chung, H.W. Kang,
J.H. Lee, and N. Spruston. 2010. A post-burst after depolarization is mediated by group i metabotropic glutamate receptor-
dependent upregulation of Ca(v)2.3 R-type calcium channels in
CA1 pyramidal neurons. *PLoS Biol.* 8:e1000534. http://dx.doi
.org/10.1371/journal.pbio.1000534

Patton, C., S. Thompson, and D. Epel. 2004. Some precautions in
using chelators to buffer metals in biological solutions. *Cell Calcium.*
35:427–431. http://dx.doi.org/10.1016/j.ceca.2003.10.006

Piedras-Rentería, E.S., and R.W. Tsien. 1998. Antisense oligonucleotides against alpha1E reduce R-type calcium currents in
cerebellar granule cells. *Proc. Natl. Acad. Sci. USA.* 95:7760–7765.
http://dx.doi.org/10.1073/pnas.95.13.7760

Ramsey, I.S., M.M. Moran, J.A. Chong, and D.E. Clapham. 2006. A
voltage-gated proton-selective channel lacking the pore domain.
Nature. 440:1213–1216. http://dx.doi.org/10.1038/nature04700

Randall, A., and R.W. Tsien. 1995. Pharmacological dissection of
multiple types of Ca^{2+} channel currents in rat cerebellar granule
neurons. *J. Neurosci.* 15:2995–3012.

Regan, L. 1993. The design of metal-binding sites in proteins.
Annu. Rev. Biophys. Biomol. Struct. 22:257–287. http://dx.doi.org/
10.1146/annurev.bb.22.060193.001353

Schneider, T., X. Wei, R. Olcese, J.L. Costantin, A. Neely, P. Palade,
E. Perez-Reyes, N. Qin, J. Zhou, G.D. Crawford, et al. 1994.
Molecular analysis and functional expression of the human type
E neuronal Ca2+ channel alpha 1 subunit. *Receptors Channels.*
2:255–270.

Sochivko, D., A. Pereverzev, N. Smyth, C. Gissel, T. Schneider, and
H. Beck. 2002. The Ca$_{(V)}$2.3 Ca(2+) channel subunit contributes
to R-type Ca($^{2+}$) currents in murine hippocampal and neocortical neurones. *J. Physiol.* 542:699–710. http://dx.doi.org/10.1113/
jphysiol.2002.020677

Soong, T.W., A. Stea, C.D. Hodson, S.J. Dubel, S.R. Vincent, and
T.P. Snutch. 1993. Structure and functional expression of a member of the low voltage-activated calcium channel family. *Science.*
260:1133–1136. http://dx.doi.org/10.1126/science.8388125

Stea, A., T.W. Soong, and T.P. Snutch. 1995. Determinants of PKC-
dependent modulation of a family of neuronal calcium channels. *Neuron.* 15:929–940. http://dx.doi.org/10.1016/0896-6273
(95)90183-3

Sun, H.S., K. Hui, D.W. Lee, and Z.P. Feng. 2007. Zn2+ sensitivity
of high- and low-voltage activated calcium channels. *Biophys. J.*
93:1175–1183. http://dx.doi.org/10.1529/biophysj.106.103333

Swartz, K.J. 2008. Sensing voltage across lipid membranes. *Nature.*
456:891–897. http://dx.doi.org/10.1038/nature07620

Tai, C., J.B. Kuzmiski, and B.A. MacVicar. 2006. Muscarinic enhancement of R-type calcium currents in hippocampal CA1 pyramidal
neurons. *J. Neurosci.* 26:6249–6258. http://dx.doi.org/10.1523/
JNEUROSCI.1009-06.2006

Tedford, H.W., and G.W. Zamponi. 2006. Direct G protein modulation of Ca$_v$2 calcium channels. *Pharmacol. Rev.* 58:837–862. http://
dx.doi.org/10.1124/pr.58.4.11

Todorovic, S.M., and C.J. Lingle. 1998. Pharmacological properties of T-type Ca^{2+} current in adult rat sensory neurons: effects
of anticonvulsant and anesthetic agents. *J. Neurophysiol.* 79:
240–252.

Tottene, A., S. Volsen, and D. Pietrobon. 2000. alpha(1E) subunits
form the pore of three cerebellar R-type calcium channels with
different pharmacological and permeation properties. *J. Neurosci.*
20:171–178.

Traboulsie, A., J. Chemin, M. Chevalier, J.F. Quignard, J. Nargeot,
and P. Lory. 2007. Subunit-specific modulation of T-type calcium
channels by zinc. *J. Physiol.* 578:159–171. http://dx.doi.org/
10.1113/jphysiol.2006.114496

Valko, M., H. Morris, and M.T. Cronin. 2005. Metals, toxicity and
oxidative stress. *Curr. Med. Chem.* 12:1161–1208. http://dx.doi
.org/10.2174/0929867053764635

Vlachová, V., H. Zemková, and L. Vyklický Jr. 1996. Copper modulation of NMDA responses in mouse and rat cultured hippocampal neurons. *Eur. J. Neurosci.* 8:2257–2264. http://dx.doi.org/
10.1111/j.1460-9568.1996.tb01189.x

Weiergräber, M., M.A. Kamp, K. Radhakrishnan, J. Hescheler, and
T. Schneider. 2006. The Ca$_{(v)}$2.3 voltage-gated calcium channel
in epileptogenesis—shedding new light on an enigmatic channel. *Neurosci. Biobehav. Rev.* 30:1122–1144. http://dx.doi.org/10
.1016/j.neubiorev.2006.07.004

Wu, L.G., J.G. Borst, and B. Sakmann. 1998. R-type Ca2+ currents evoke transmitter release at a rat central synapse. *Proc. Natl. Acad. Sci. USA.* 95:4720–4725. http://dx.doi.org/10.1073/pnas.95.8.4720

Yasuda, R., B.L. Sabatini, and K. Svoboda. 2003. Plasticity of calcium channels in dendritic spines. *Nat. Neurosci.* 6:948–955. http://dx.doi.org/10.1038/nn1112

Zamponi, G.W. 2005. Voltage-Gated Calcium Channels. Kluwer Academic/Plenum Publishers, New York. 391pp.

Zamponi, G.W., E. Bourinet, and T.P. Snutch. 1996. Nickel block of a family of neuronal calcium channels: subtype- and subunit-dependent action at multiple sites. *J. Membr. Biol.* 151:77–90. http://dx.doi.org/10.1007/s002329900059

Zhang, J.F., A.D. Randall, P.T. Ellinor, W.A. Horne, W.A. Sather, T. Tanabe, T.L. Schwarz, and R.W. Tsien. 1993. Distinctive pharmacology and kinetics of cloned neuronal Ca^{2+} channels and their possible counterparts in mammalian CNS neurons. *Neuropharmacology.* 32:1075–1088. http://dx.doi.org/10.1016/0028-3908(93)90003-L